ORGANOMETALLICS

pubs.acs.org/Organometallics

Article

Well-Defined Dinuclear Copper(II) Complexes with Distorted Coordination Environments Promote C−N Coupling Reactions via Tandem Cu^{II}–Cu^{III} Redox Catalysis

Lorenzo Marchi, Luca Terraneo, Gabriele Vaccari, Markus Steiner, Ritik Singhal, Laura Pigani, Carlo Castellano, Francesco Demartin, Philipp Pascal Nievergelt, André Alker, Frank Stowasser, Serena Maria Fantasia,* and Luca Rigamonti*

Cite This: *Organometallics* 2025, 44, 2807−2819

Read Online

ACCESS | Metrics & More | Article Recommendations | Supporting Information

ABSTRACT: Dinuclear copper(II) complexes of the general formula $[Cu_2(\mu\text{-}L^n)_2]$ (**1**−**6**) with shortened salen-type N_2O_2 tetradentate Schiff base ligands named $H_2sal(X)ben$ ($\mathbf{H_2L^n}$, n = 1−7, X = H, 2-OMe, 4-OMe, 2-Cl, 4-Cl, 2,6-diOMe, 2,4,6-triOMe, respectively) revealed to be efficient and selective catalysts for Ullmann-type C−N coupling reactions under relatively mild conditions. These compounds display a distorted metal coordination environment, intermediate between tetrahedral and square planar, as shown by single-crystal X-ray diffraction, caused by the one-carbon bridge linking the iminic nitrogen atoms. This peculiar feature suggests that the metal ions can easily modulate and adapt to different redox states, evoking their potential as efficient catalysts. In fact, they revealed excellent performance in the Ullmann-type C−N coupling reaction, being reactive toward a wide range of *N*-nucleophiles and successfully coupling sterically hindered and electronically deactivated aryl iodides. Mechanistic studies support a 2-electron oxidative addition/reductive elimination event taking place on one copper(II) center, while the other acts as an electron reservoir to assist the redox process. Noteworthy, catalysts **1**−**6** are easily prepared from nonexpensive starting materials and are stable to air and moisture, characteristics that render them a very attractive alternative to classic *in situ*-generated catalytic systems, notably in the context of industrial applications.

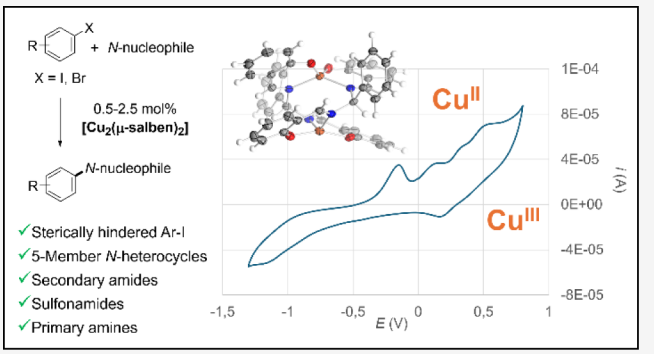

INTRODUCTION

Copper-catalyzed C−N coupling reactions have become, in the past decade, a fundamental tool in the synthesis of complex molecules. Initially reported in its substoichiometric version by Ullmann and Goldberg at the beginning of the last century,[1,2] it has developed into an efficient catalytic reaction in the last 30 years. Thanks to the efforts of many research groups, the identification of a wide number of supporting ligands has allowed for the use of reduced amount of copper, milder reaction conditions, and wider functional group tolerance and substrate scope.[3,4] Notably, the last generation oxalamide-type ligands reported by Ma[5−8] and Hartwig[9,10] granted access to the coupling of (hetero)aryl chloride substrates, while diamine aryl ligands from Buchwald[11,12] and a picolinylhydrazide ligand from König and Hillenbrand[13] enabled the coupling of aryl bromides at room temperature (RT). These features, together with the abundance of copper and its low price, have contributed to transform the copper-catalyzed C−N coupling into an attractive alternative to the related palladium-catalyzed methodology.[14] The latter has dominated the cross-coupling field for the last 30 years, fueled by intensive research on ligands as well as on precatalyst design. In particular, the use of well-defined palladium complexes bearing the desired ancillary ligands boosted the performance of catalytic systems and is nowadays recognized as the standard approach to palladium-catalyzed coupling reactions.[15,16] On the other hand, copper-catalyzed protocols still mainly rely on the *in situ* approach, with very few well-defined catalysts being reported in literature.[17−20] Unfortunately, directly mixing the copper source and the ligands in the reaction mixture with the other reagents leads to poor control of the number of coordinated ligands and metal oxidation state, potentially giving rise to a considerable amount of inactive copper species. Additional

Received: October 15, 2025
Revised: October 31, 2025
Accepted: November 12, 2025
Published: November 17, 2025

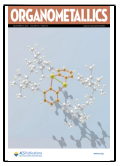

https://doi.org/10.1021/acs.organomet.5c00412
Organometallics 2025, 44, 2807−2819

Scheme 1. H_2L^n Ligands (n = 1−7) and Related Copper(II) Complexes 1−6; RX Code Identifies Compounds for Which X-ray Crystal Structure is Available

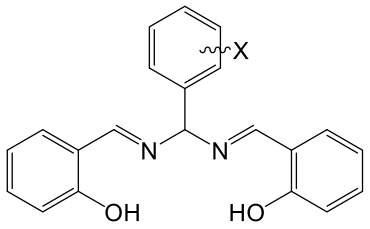

Ligand

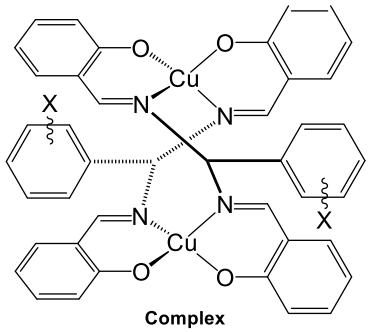

Complex

X	Ligand	Complex
H	H_2L^1	**1** (RX)
2-OMe	H_2L^2 (RX)	**2** (RX)
4-OMe	H_2L^3	**3** (RX)
2-Cl	H_2L^4	**4** (RX)
4-Cl	H_2L^5	**5** (RX)
2,6-diOMe	H_2L^6 (RX)	**6**
2,4,6-triOMe	H_2L^7 (RX)	-

drawbacks include the cost and purification efforts associated with the use of a large (typically a 5−10-fold) excess of ligands and the instability to moisture and oxygen of copper(I) salt precursors with tendence to disproportionation/oxidation.[21] In this context, the use of well-defined and air-stable copper(II) complexes would bring about considerable improvements to the stability and activity of the catalytic systems.

In 2000, a report by Pasini disclosed the synthesis and characterization of copper(II) complexes bearing X-substituted *bis*(salicylidene)phenylmethanediamine Schiff bases H_2sal(X)-ben ($\mathbf{H_2L^n}$, see Scheme 1 for X groups employed in this paper and numbering correspondence),[22] functionalized on the central aryl ring with different substituents X.[23] They behave as dianionic N_2O_2 tetradentate ligands once the phenolic groups are deprotonated.[22,24−27] Differently from the most-known H_2salen (*N,N′-bis*(salicylidene)-ethylenediamine),[28] where the iminic nitrogen atoms of the condensed salicylaldehyde (salH) are connected through a two-carbon-atom ethylene bridge (en), $\mathbf{H_2L^n}$ ligands have only one carbon atom linking the two salH moieties. On the other hand, they possess the same donor set and they can be considered shortened salen-type Schiff bases. Because of the one-carbon bridge, which would generate a high ring strain in the four-membered metallocycle (M−N−C−N) of a hypothetical mononuclear complex as seen in salen does, $\mathbf{H_2L^n}$ selectively form not only dinuclear compounds $[M_2(\mu\text{-}L^n)_2]$ with divalent ions like copper(II)[22] and cobalt(II)[24] but also tetranuclear clusters $[M_4(\mu_3\text{-}O)_2(\mu_2\text{-}L^n)_4]$ with the trivalent ion iron(III) with triply bridging oxido ions.[27] The interesting aspect of $[Cu_2(\mu\text{-}L^n)_2]$ derivatives (**1−6**, see Scheme 1), which led us to focus our attention on them, is the distorted coordination environment of the copper(II) ions, as outlined in the crystal structure at 293 K of **1**·0.5*i*Pr_2O reported by Pasini[22] (see below for further details). We speculated that the intermediate geometry of the copper center between tetrahedral and square planar could enable straightforward and selective access to different oxidation states, such as Cu^I and Cu^{III} that are typical of the C−N coupling catalytic cycle.[17,18,29,30] The ligand flexibility would play a key role in stabilizing these active species, controlling and minimizing the formation of off-path, unproductive copper compounds, an aspect that was already highlighted by Taillefer in his studies on the catalytic activities of various ligand classes.[31−33] Furthermore, the proximity of the two metal centers could give rise to metastable intermediates with mixed valence ions, ultimately enhancing catalytic behaviors.

The salben ligands have been mainly studied in the context of the magnetic properties of the corresponding oligonuclear clusters with paramagnetic metal ions,[22,24−27] while the reports on the catalytic activity of their metal complexes are scarce[34,35] with no report on direct C−N coupling. On the other hand, it is known that copper(I) complexes with oligonuclear Schiff bases can catalyze the Ullmann-type C−N coupling between aryl halides (in particular, iodide) and nucleophiles.[3,31,36]

We here present the catalytic performance of the copper salben complexes **1−6** in the C−N coupling reaction of aryl halides with various *N*-nucleophiles,[37] and we disclose mechanistic studies that shed light on the copper species involved in the catalytic cycle.

RESULTS AND DISCUSSION

Synthesis and Structural Features of Ligands and Complexes. $\mathbf{H_2L^n}$ can be obtained from the reaction of the precursor H_3salmp (*N,N′-bis*(salicylidene)-2-hydroxyphenyl-methanediamine)[38] by replacing the central salH moiety with an X-substituted benzaldehyde (see Scheme S1 in Supporting Information (SI)).[23] In this work, we applied this synthetic procedure for obtaining not only the already-known H_2sal-(X)ben with X = H ($\mathbf{H_2L^1}$), 2-OMe ($\mathbf{H_2L^2}$), 4-OMe ($\mathbf{H_2L^3}$), 2-Cl ($\mathbf{H_2L^4}$), and 4-Cl ($\mathbf{H_2L^5}$)[22,24] but also the new derivatives with X = 2,6-diOMe ($\mathbf{H_2L^6}$) and 2,4,6-triOMe ($\mathbf{H_2L^7}$), aiming at studying the effect of different substituents on the structural and catalytic features of the corresponding dinuclear complexes. Derivatives $\mathbf{H_2L^4}$, $\mathbf{H_2L^6}$, and $\mathbf{H_2L^7}$ could be obtained as single crystals suitable for X-ray diffraction by slow evaporation of a $CHCl_3$ solution or diffusion of *n*-hexane into a DCM solution, and the determined structures confirm the nature of the ligands (see Table S1, full structural description and Figure S1 in SI).

The complexation was performed following the procedure reported by Pasini et al.[22] in absolute EtOH at RT in the presence of NEt_3 as a deprotonating base and copper(II) acetate as the metal source. The reaction time varies from ligand to ligand (see Experimental Section in SI for further details), and all the procedures were optimized to ensure the highest purity of the final $[Cu_2(\mu\text{-sal(X)ben})_2]$ compounds (**1−6**), checked through elemental analysis, infrared (IR) spectroscopy, and mass spectrometry. The copper(II) species **1−6** are also air-stable, allowing easy storage and handling under ambient conditions. Any attempt to obtain the copper(II) complex with $\mathbf{H_2L^7}$ failed since the hypothetical compound **7** tends to hydrolyze in solution to $[Cu(salim)_2]$ (Scheme S1 in SI), as clearly highlighted by IR through the appearance of N−H stretching at 3300 cm^{-1}, independently from the reaction conditions.

https://doi.org/10.1021/acs.organomet.5c00412
Organometallics 2025, 44, 2807−2819

As stated above, the X-ray crystal structure of **1**·0.5*i*Pr_2O was reported by Pasini et al.,[22] and we could now obtain two new solvatomorphs **1**·0.4*n*-hexane and **1**·1.15*n*-hexane by diffusion of *n*-hexane into concentrated solutions of the title complex in DCM and THF, respectively. Furthermore, crystal structures of **2**, **3**·0.5$CHCl_3$, **4**·0.5*n*-hexane, and **5**·0.5*n*-hexane could be obtained upon isolation of single crystals from diffusion of *n*-hexane into DCM, $CHCl_3$, DCM, and DCM solutions, respectively (see Table S1 and full structural description in SI). In all cases, the dinuclear nature of the copper compounds was undoubtedly confirmed (see Figure 1 and Figure S2 in SI), and the relevant structural parameters are reported in Table 1 and Table S2 in SI.

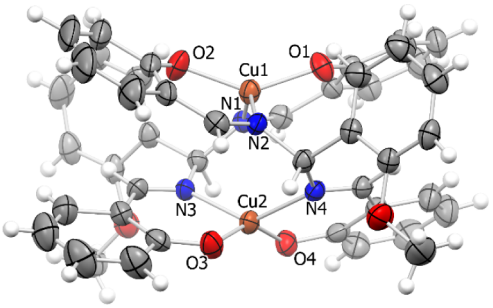

Figure 1. Perspective view of the crystal structure of **2** with main atom numbering; ellipsoids are reported at the 50% probability, while hydrogen atoms are drawn as idealized spheres; color code: Cu = orange, O = red, N = blue, C = gray, H = white.

The coordination of the copper(II) ions can be outlined by the dihedral angle θ between the two least-squares (l.s.) planes described by copper, oxygen, and nitrogen atoms of each salicylaldehydato fragment, where $\theta = 90°$ for the tetrahedral coordination, while $\theta = 0°$ in a square planar environment. Alternatively, the geometry index τ_4 introduced by Hauser et al. can be calculated and employed to compare these congener complexes, since $\tau_4 = 1$ for tetrahedral while $\tau_4 = 0$ for square planar.[39] Indeed, all metal ions reside in a highly distorted environment with a geometry intermediate between square planar and tetrahedral (or between square pyramidal and trigonal bipyramidal for copper(II) ions involved in short dimeric interactions; see Table 1 and SI for further details). These distorted geometries arise from the bridging N−C−N between the two metal atoms, and this imparts a high flexibility to the ions that can modify their surroundings, for example, once in solution through interaction with solvent or base, and via reduction or oxidation to copper(I) and copper(III), respectively. This is also clear when looking at coordination bond distances, which are not elongated with respect to what is expected as in the case of [Cu(salen)],[40] but are quite short being around 1.87 Å for Cu−O and 1.98 Å for Cu−N. These data are particularly relevant in view of the catalytic performances of the complexes, since it has been predicted that copper-catalyzed Ullmann-type C−N coupling reactions should be boosted when the Cu−L coordination bond distances between the Cu and the ligand are below the threshold of 2.07 Å.[41]

The electrochemistry of **1**−**5** in solution was studied, aiming at investigating the possibility of reduction or oxidation of the metal centers, together with the reversibility of those processes.

Table 1. Coordination Distances (Å), Together with Distortion Parameters θ (°), for 1·0.5*i*Pr_2O,[22] 1·0.4*n*-hexane, 1·1.15*n*-hexane, 2, 3·0.5$CHCl_3$, 4·0.5*n*-hexane, and 5·0.5*n*-hexane

	1·0.5*i*Pr_2O[a]	1·0.4*n*-hexane	1·1.15*n*-hexane	2	3·0.5$CHCl_3$	4·0.5*n*-hexane	5·0.5*n*-hexane
Cu1−O1	1.870(3)	1.8780(18)	1.881(3)	1.8617(19)	1.883(2)	1.8802(16)	1.880(3)
Cu1−O2	1.868(3)	1.8686(18)	1.881(3)	1.8760(19)	1.874(2)	1.8876(17)	1.875(3)
Cu1−N1	1.994(3)	1.996(2)	1.981(3)	1.985(2)	1.987(2)	1.9896(19)	1.989(3)
Cu1−N2	1.984(3)	1.979(2)	1.981(3)	1.994(2)	1.991(2)	1.9989(18)	1.995(3)
Cu2−O3	1.903(3)	1.9114(19)	1.906(2)	1.870(2)	1.9138(19)	1.8874(15)	1.906(3)
Cu2−O4	1.892(3)	1.8956(19)	1.889(2)	1.8672(19)	1.9003(19)	1.8699(16)	1.897(3)
Cu2−N3	2.034(3)	2.027(2)	2.023(3)	1.964(2)	2.016(2)	1.9866(18)	2.017(3)
Cu2−N4	2.004(3)	2.001(2)	1.998(3)	1.968(2)	2.011(2)	1.9852(19)	1.999(3)
Cu3−O5	1.899(3)	1.9074(19)	1.910(2)	-	1.910(2)	-	1.903(3)
Cu3−O6	1.890(3)	1.8976(19)	1.895(2)	-	1.893(2)	-	1.901(3)
Cu3−N5	2.029(3)	2.027(2)	2.031(3)	-	2.017(2)	-	2.018(3)
Cu3−N6	2.001(3)	1.999(2)	2.000(2)	-	1.997(2)	-	2.007(3)
Cu4−O7	1.884(3)	1.879(2)	1.878(2)	-	1.883(2)	-	1.878(3)
Cu4−O8	1.889(3)	1.875(2)	1.875(2)	-	1.872(2)	-	1.884(3)
Cu4−N7	1.985(4)	1.984(2)	1.988(3)	-	1.989(2)	-	1.988(3)
Cu4−N8	1.996(4)	1.994(2)	1.976(3)	-	1.991(2)	-	1.994(3)
Cu2···O5	2.520(4)	2.452(2)	2.392(3)	-	2.392(2)	-	2.407(4)
Cu3···O3	2.452(4)	2.385(2)	2.415(3)	-	2.413(2)	-	2.414(3)
Cu1···Cu2	3.215(1)	3.2165(6)	3.247(1)	3.1618(7)	3.1076(7)	3.1478(5)	3.046(10)
Cu3···Cu4	3.242(1)	3.2611(7)	3.234(1)	-	3.0536(7)	-	3.112(10)
Cu2···Cu3	3.181(1)	3.1175(6)	3.113(1)	-	3.1502(6)	-	3.1581(8)
θ, τ_4 Cu1	56.04, 0.57	55.51, 0.57	55.96, 0.57	57.86, 0.59	53.35, 0.55	54.88, 0.56	46.82, 0.48
θ, τ_4 Cu2	53.29, 0.50	53.10, 0.50	53.67, 0.49	55.20, 0.56	47.94, 0.44	52.80, 0.53	45.18, 0.43
θ, τ_4 Cu3	53.05, 0.49	53.96, 0.49	53.96, 0.50	-	46.37, 0.44	-	48.33, 0.45
θ, τ_4 Cu4	55.76, 0.57	56.71, 0.58	56.03, 0.57	-	50.29, 0.51	-	51.86, 0.43

[a]Original atom numbering adapted for comparison with new crystallographic data.

https://doi.org/10.1021/acs.organomet.5c00412
Organometallics 2025, 44, 2807−2819

Figure S3 in SI shows the voltammograms obtained for **1**−**5** in DMSO. In all cases, it is possible to observe two separate peaks at negative potentials associated with $Cu^{II} \rightarrow Cu^{I}$ reduction processes (Table S3 in SI for the relative values of the peak potentials), which are reversible (see SI for further details). Under the measurement conditions tested here, i.e., RT with no additive in solution, we could not observe any oxidation peak to copper(III) in the positive potential region. Of note, cyclic voltammetry (CV) measurements under catalytic conditions showed different behaviors (see below for further discussion).

Catalytic Performances. Due to the relevance of the azole motif in pharmaceutically active molecules, we set to explore the catalytic activity of **1**−**6** in the coupling of pyrrole with iodobenzene (PhI) (Scheme 2).[42,43] Indeed, the copper-

Scheme 2. Model Reaction Used for Optimization and Mechanistic Studies

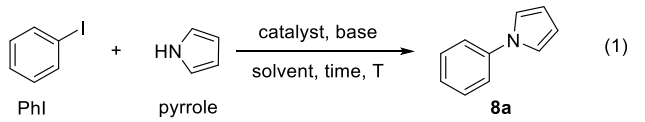

catalyzed coupling of *N*-heterocycles proved to be a challenging one, generally requiring 5 mol % or more of a copper source to achieve good conversions.[31,32,36,44−48] The advent of oxalamide ligands allowed to reduce the copper amounts needed for such couplings to 2 mol %,[49,50] while a loading of 1 mol % was enabled by using a 10-fold excess of *trans*-cyclohexyl-1,2-diamine.[51] Interestingly, a recent report shows that a well-defined copper(II) phthalocyanine complex also enables the efficient coupling of azoles at a 1 mol % catalyst loading.[19]

A screening of reaction conditions in the presence of 0.5 mol % of **1** identified MeCN and Cs_2CO_3 (2 equiv) as the optimal solvent/base combination. The highest conversion was obtained using pyrrole as the limiting reagent and refluxing the reaction mixture (82 °C) for 16 h (see Tables S4 and S5 in SI for further details). Under these conditions, the 1-phenylpyrrole **8a** was formed in practical quantitative yield (98% as judged by ^{1}H NMR spectroscopy, Table 2, entry 1, dimethylsulfone Me_2SO_2 as the internal standard). The benefit of using a well-defined catalyst is confirmed by the lower performance of the *in situ* protocol. Indeed, the use of a copper source in combination with the H_2L^1 ligand in a 1:1 ratio

Table 2. Catalytic Performances of 1−6 for the Coupling of PhI with Pyrrole to 8a, Eq 1 in Scheme 2, in MeCN, Cs_2CO_3 as Base and at 82 °C

Entry	Catalyst	Catalyst loading (mol %)	*t* (h)	Yield %[a]
1	**1** (X = H)	0.5	16	98
2	$Cu(OAc)_2$ + H_2L^1	1.0	16	67
3	Cu_2O + H_2L^1	0.5	16	79
4	**1** (X = H)	0.25	48	84
5	**2** (X = 2-OMe)	0.5	16	94
6	**3** (X = 4-OMe)	0.5	16	90
7	**6** (X = 2,6-diOMe)	0.5	16	96
8	**4** (X = 2-Cl)	0.5	16	92
9	**5** (X = 4-Cl)	0.5	16	96

[a]^{1}H NMR yield, Me_2SO_2 as internal standard; conversion not determined.

achieved only 67% yield with $Cu(OAc)_2$ (Table 2, entry 2) and 79% yield with Cu_2O (Table 2, entry 3) at 1 mol % copper loading. Increasing the ligand:copper source ratio has no effect on the reaction yield (Table S6 in SI), suggesting that saturation of the copper coordination sites is reached with just one equivalent of ligand. By reducing the loading of **1** to 0.25 mol %, an excellent 84% yield could still be achieved after 48 h (Table 2, entry 4). To the best of our knowledge, this result represents the lowest turnover number (TON) achieved so far in the coupling of PhI with pyrrole.

The catalytic activity of **2**−**6**, bearing the substituted salben ligands, was tested (Table 2, entries 5−9) and resulted in excellent activity for all of them: **5** and **6** afforded the product in 96% yield, followed by **2** at 94% yield, **4** at 92% yield, and **3** at 90% yield. A trend connected with the stereoelectronic properties of the substituent X on the central aryl ring does not seem to be evident, though data analysis may be hampered by the small variation in yield compared to the experimental error. On the other hand, the influence of parameters such as catalyst solubility or structural distortions that are able to alter the redox properties cannot be excluded.

The catalytic activity of **1** was then further profiled. Importantly, among the family of copper-salben complexes, **1** is the most cost-effective derivative as it is synthesized from the least-expensive unsubstituted benzaldehyde. The reaction scope was first explored with respect to the aryl iodide, and it was found that both electron-withdrawing groups such as nitrile and electron-donating groups such as methoxide are well tolerated by the catalyst in any position of the ring (**8b**−**g**, Scheme 3). 1-Iodo-3-methoxybenzene can be coupled with 0.5 mol % catalyst to afford **8b** in 94% yield, while 3-iodobenzonitrile requires 0.75 mol % of catalyst loading to

Scheme 3. Coupling of Aryl Iodides with 5-Member *N*-Heterocycles[a]

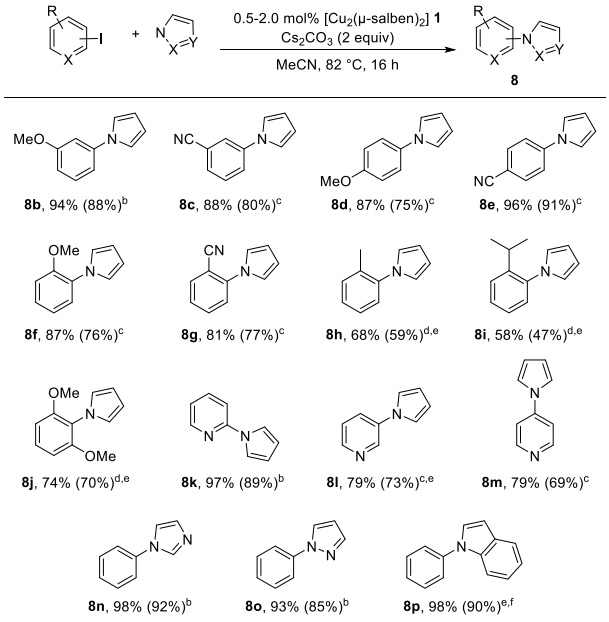

[a]For detailed reaction conditions, see the SI. X = Y = C for **8b**−**8m**; X = C, Y = N for **8n**; X = N, Y = C for **8o**; X = Y = C_6H_6 for **8p**. ^{1}H NMR yields reported (Me_2SO_2 as internal standard), isolated yields given in brackets; [b]0.5 mol % **1**; [c]0.75 mol% **1**; [d]1.0 mol % **1**; [e]48 h reaction time; [f]2.0 mol % **1**.

https://doi.org/10.1021/acs.organomet.5c00412
Organometallics 2025, 44, 2807−2819

Scheme 4. Coupling of Aryl Iodides with Amines, Amides, and Sulfonamides[a]

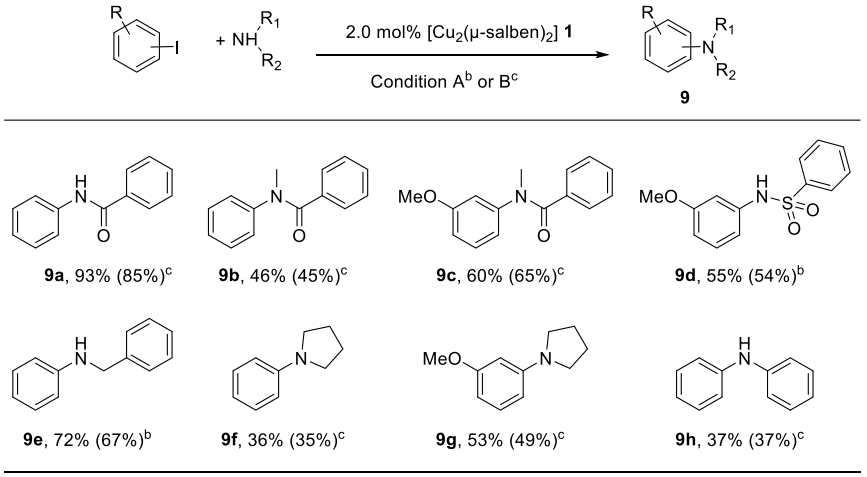

[a]For detailed reaction conditions, see the SI. ^{1}H NMR yields reported (Me_2SO_2 as internal standard), isolated yields given in brackets; [b]MeCN, 2 equiv Cs_2CO_3, 82 °C, 48 h; [c]DMSO, 3 equiv K_3PO_4, 120 °C, 48 h.

Scheme 5. Coupling of Aryl Bromides with *N*-Nucleophiles[a]

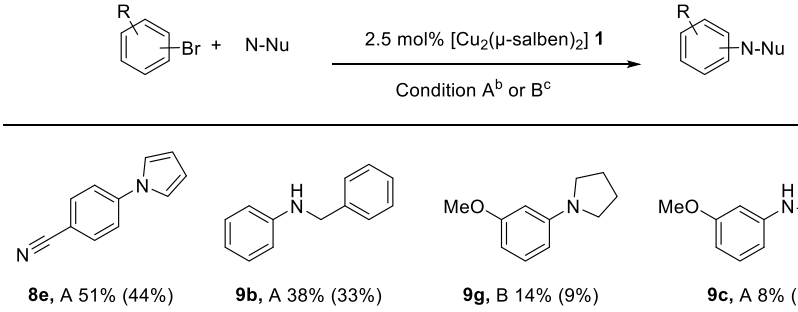

[a]For detailed reaction conditions, see the SI. ^{1}H NMR yields reported (Me_2SO_2 as internal standard), isolated yields given in brackets; [b]MeCN, 2 equiv Cs_2CO_3, 82 °C, 48 h; [c]DMSO, 3 equiv K_3PO_4, 120 °C, 48 h.

afford product **8c** in 88% yield. Similarly, substitution of the *para* or *ortho* position with either an OMe or CN group requires a slightly higher amount of catalyst (0.75 mol %) to achieve yields in the 81−96% range for products **8d**−**8g**.

Ortho-substituted substrates pose a particular challenge due to their unfavorable steric properties.[52−54] Encouraged by the promising results obtained with compounds **8f** and **8g**, we explored the reactivity of additional *ortho*-substituted substrates. Pleasantly, 1-iodo-2-methylbenzene, 1-iodo-2-isopropylbenzene, and 2-iodo-1,3-dimethoxybenzene efficiently coupled with pyrrole with 1.0 mol % catalyst, and after 48 h, the coupling products **8h**, **8i**, and **8j** were obtained in 68%, 58%, and 74%, respectively. These results are noteworthy, particularly the coupling of the di-*ortho*-substituted 2-iodo-1,3-dimethoxybenzene, which, to the best of our knowledge, is unprecedented.

The catalyst also demonstrated excellent performance with iodopyridines, with 2-iodopyridine affording 97% yield of **8k** at 0.5 mol % catalyst loading and 3- and 4-iodopyridines requiring slightly higher catalyst loading (0.75 mol %) to produce **8l** and **8m** in 79% yields.

Other 5-member *N*-based heteroaromatics such as imidazole and pyrazole are efficiently coupled at 0.5 mol % catalyst loading affording products **8n** and **8n** in excellent yields, while quantitative coupling of indole, a notoriously challenging substrate, with PhI (product **8p**) is achieved with 2 mol % catalyst loading and 48 h reaction time. These results position **1** among the most efficient catalysts reported to date for the coupling of aryl iodides with *N*-heterocycles.[4,55]

We then explored the tolerance of the catalytic system to other classes of *N*-nucleophiles and found that the catalyst is effective in the coupling of a wide range of substrates at 2 mol % loading (Scheme 4). Additional optimization of the reaction conditions showed that for acetamides, pyrrolidine, and aniline, the coupling worked best in DMSO with 3 equiv of K_3PO_4 as base at 120 °C.

Benzylamide displays excellent reactivity toward PhI affording **9a** in 93% yield, while the yield dropped to 46% when the secondary amide *N*-methylbenzamide was used (product **9b**). On the other hand, coupling of *N*-methylbenzamide with 3-methoxyiodobenzene performed better, affording **9c** in 60% yield. Sulfonamide is also a competent *N*-nucleophile and undoubtedly of interest,[31,48,56] and it couples to 3-methoxy-1-iodobenzene to afford **9d** in 55% yield. In the class of alkyl amines, benzylamine displays good reactivity allowing the formation of **9e** in 72% yield, while when pyrrolidine is used, the efficiency of the catalytic system diminishes, affording products **9f** and **9g** in 36% and 53% yield, respectively. Similarly, the coupling of aniline under these conditions returned a modest yield of 37% for **9h**, in line with

https://doi.org/10.1021/acs.organomet.5c00412
Organometallics 2025, 44, 2807−2819

Scheme 6. Radical Trap Experiment

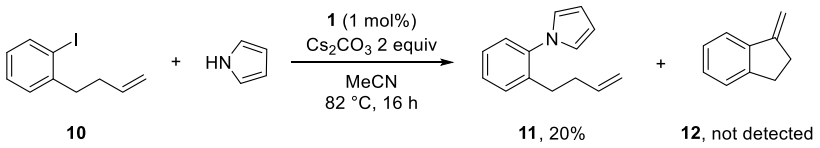

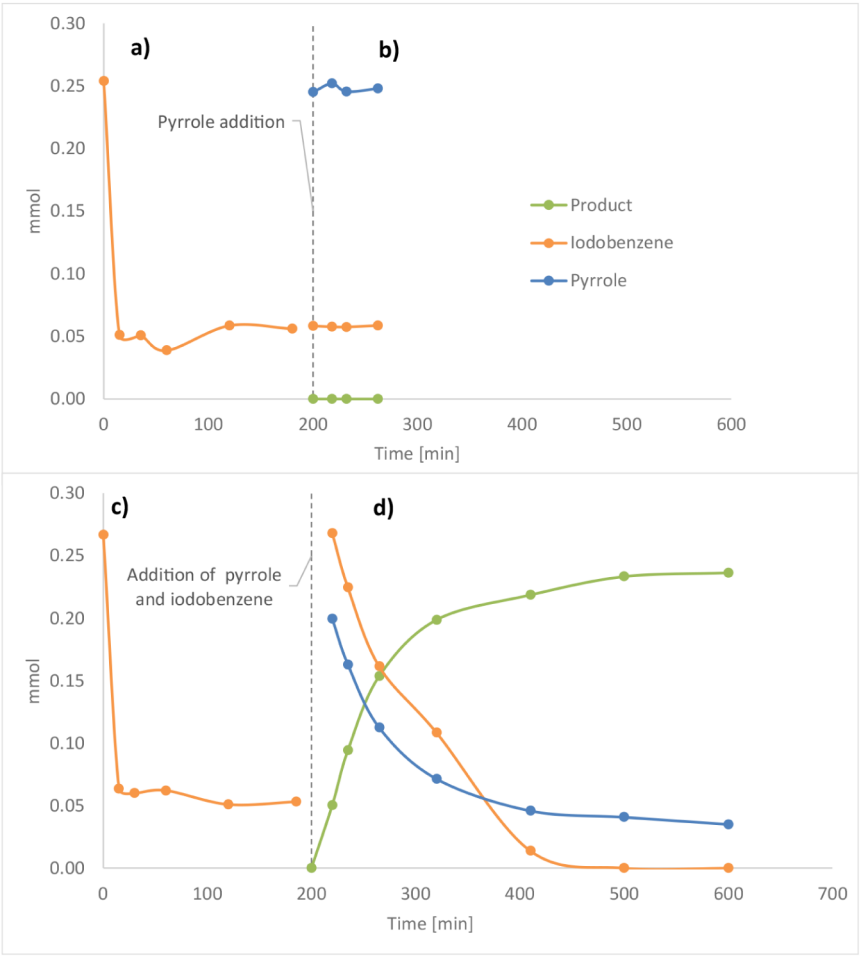

Figure 2. a) PhI content monitored during the reactions with base and b) reagents and product evolution of a) after the addition of 2 equiv of pyrrole; c) PhI content monitored during the reactions with base and d) reagents and product evolution of c) after the addition of 2 equiv of pyrrole and PhI.

the known challenge posed by aniline coupling partners in copper-catalyzed reactions.[8,11−13,57,58]

Next, the reactivity of **1** was evaluated with a series of aryl bromides (Scheme 5). Generally, aryl bromides displayed lower reactivity, with 2.5 mol % catalyst needed to couple 4-cyano-1-bromobenzene with pyrrole in a moderate 51% yield (**8e**). More challenging nucleophiles such as benzylamine, pyrrolidine, and sulfonamide, which already required higher catalyst loadings to react with aryl iodides (Table S7 in SI), coupled with aryl bromides in poor yields (38%, 14%, and 8% for **9b**, **9g**, and **9c**, respectively). Aryl chlorides showed no observable coupling under the same reaction conditions.

Importantly, the whole reaction scope was explored on a 1.3 mmol scale (limiting reagent); to prove the scalability of the catalytic system, we performed the coupling to **8g** and **9c** on a 25.8 mmol scale (scale-up factor = 20, see SI for the experimental procedure). Pleasantly, both products were isolated in very similar amounts, with **8g** affording 71% yield (vs 77% on 1.3 mmol) and **9c** affording 62% yield (vs 65% on 1.3 mmol).

Mechanistic Insights. The remarkable activity of **1** toward a broad range of *N*-nucleophiles and especially toward *ortho*-substituted aryl iodides was intriguing and prompted us to explore the reaction mechanism. It is well accepted that when using first-generation ligands, copper-catalyzed C−X coupling proceeds via a copper(I)/copper(III) mechanism.[17,29,30,59−61] Recently, it was demonstrated that second-generation dianionic oxalamide ligands promote a noncanonical copper(II)/copper(III) mechanism by accommodating the extra charge of the formal copper(IV) catalytic species expected from an oxidative addition-type mechanism.[10,18]

We first explored the possibility of a radical mechanism or radical formation by performing the radical trap experiment reported by Hartwig.[18] We synthesized the alkene-containing aryl iodide **10** (see SI for the experimental procedure) and reacted it with pyrrole under the optimized catalytic reaction

https://doi.org/10.1021/acs.organomet.5c00412
Organometallics 2025, 44, 2807−2819

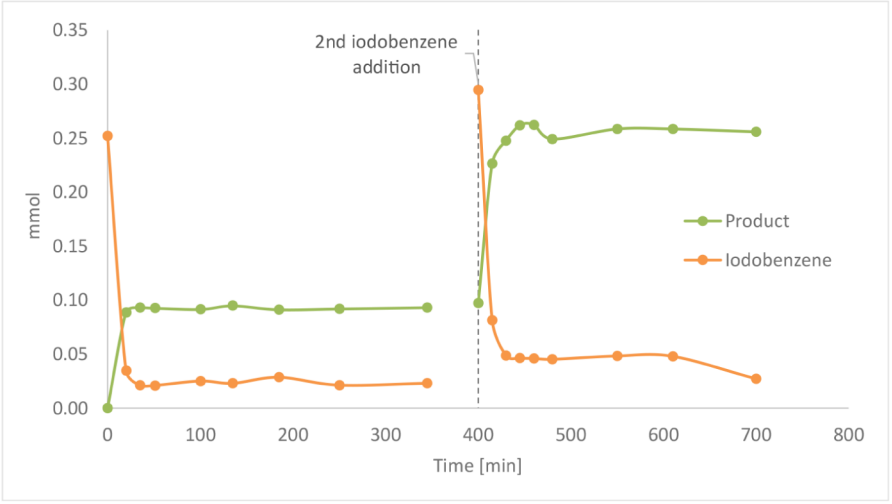

Figure 3. Single turnover experiment for PhI followed by the addition of extra PhI.

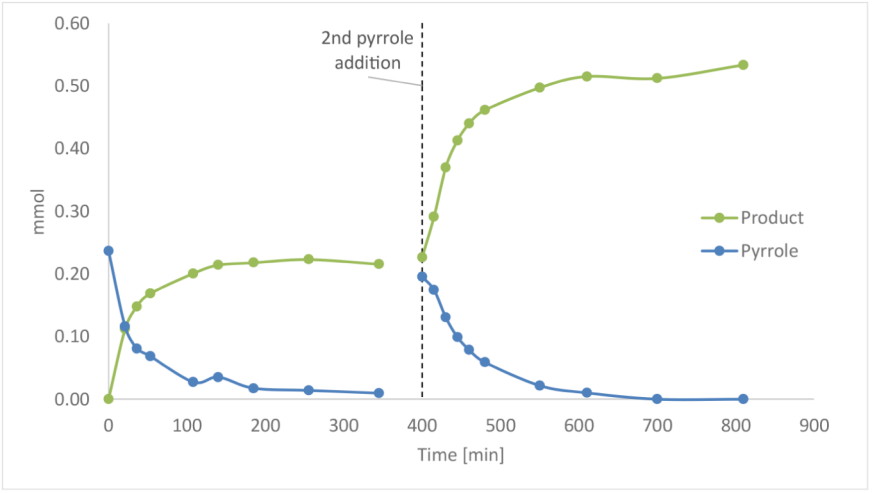

Figure 4. Single turnover experiment for pyrrole.

conditions (Scheme 6). We observed the formation of about 20% coupling product **11** and no formation of the cyclized product **12** (by quantitative ^{1}H NMR, mostly unreacted **10** remaining), suggesting that indeed a nonradical mechanism is operative, and no radical species are formed.

As reported above, CV measurements of **1** in DMSO show two reversible reduction peaks, which led us to first hypothesize facile reduction to copper(I) as catalytically active species, followed by the well-known Cu^I/Cu^{III} cycle. However, the identification of the actual reducing agent was not obvious: if we consider the model reaction depicted in Scheme 2, pyrrole is known to oxidize only with specific reagents and reaction conditions,[62] and PhI is expected to oxidize the metal center via oxidative addition paths. To shed light on the activation mechanism of **1**, we performed stoichiometric reactions between **1** and the coupling partners as single-turnover experiments. The coupling between PhI and pyrrole (Scheme 2) was used for the mechanistic studies. To ensure solubility of the coupling partners, the catalyst, and the product in the reaction mixture, all the experiments aimed at discerning the reaction mechanism were performed in DMSO using K_3PO_4 as the base (3 equiv), a combination that ensured full conversion to the target product at 120 °C after 16 h with 0.5 mol % of **1** (84% isolated yield).

Mixing **1** with pyrrole (2 equiv) and K_3PO_4 (10 equiv) in DMSO does not trigger any pyrrole consumption after 3 h at 120 °C, while when PhI (2 equiv) is mixed with **1** and K_3PO_4 (10 equiv), only 20% of it is left after 15 min. If PhI is mixed with **1** in the absence of base, its consumption is still observed, albeit at a slower rate (50% after 3 h, Figure S34 in SI).

An LC−MS analysis of the reaction mixture showed the presence of $\mathbf{H_2L^1}$ (m/z 329.2 $[M - H]^-$) along with the formation of a new compound with a mass corresponding to the salben ligand plus a phenyl fragment (m/z 405.2 $[M - H]^-$) (Figure S33 in SI). We can hypothesize the formation of the phenyl ether of the salben ligand via the oxidative addition of PhI to **1** followed by the reductive elimination of the phenolate and aryl fragments. Importantly, the oxidative addition of aryl halides onto a copper(II) center has recently been disclosed as a viable mechanistic pathway for copper-catalyzed C−O and C−N couplings.[10,18]

As described above, PhI is consumed when mixed with **1** and K_3PO_4 (Figure 2a); subsequent addition of pyrrole (2 equiv) does not lead to product formation (Figure 2b), supporting the consumption of PhI in an irreversible reaction.

https://doi.org/10.1021/acs.organomet.5c00412
Organometallics 2025, 44, 2807−2819

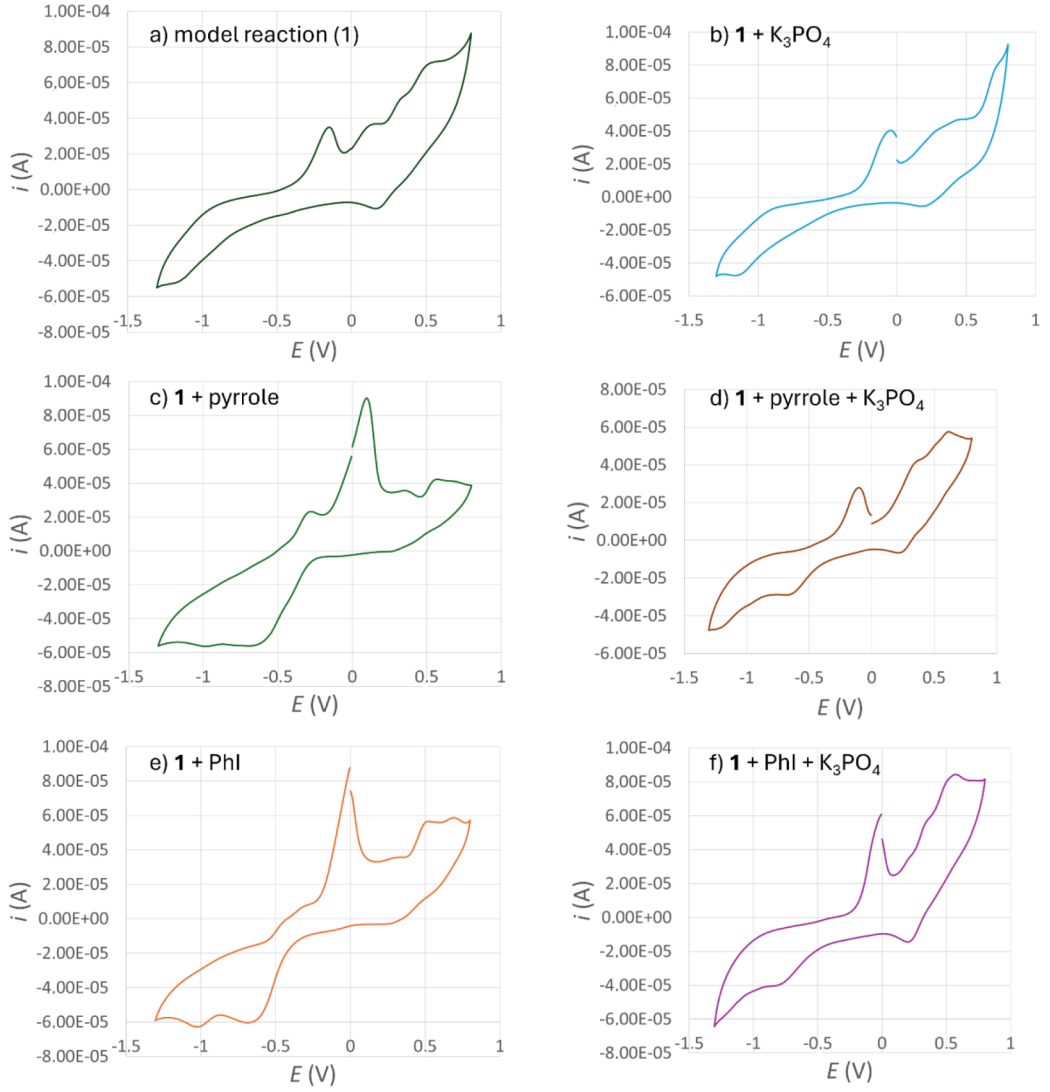

Figure 5. CV measurements performed after heating the reaction mixture at 80 °C for 4 h and then adding $LiClO_4$ up to a concentration of 0.1 mol L^{-1} in DMSO, ν = 100 mV/s: a) model reaction (1); b) **1** + K_3PO_4; c) **1** + pyrrole; d) **1** + pyrrole + K_3PO_4; e) **1** + PhI; and f) **1** + K_3PO_4 + PhI.

On the other hand, when both 2 equiv of pyrrole and PhI were added, the product was formed in 90% yield (Figure 2c). The single-turnover experiment was then repeated by mixing all the components at once with 1 equiv of **1**, 2 equiv of PhI, excess pyrrole, and excess base (Figure 3). Under these conditions, the formation of the coupling product was observed but only in 35% yield. Further addition of PhI (2 equiv) produced an increase in yield to 60%. The results are compatible with a scenario where the formation of the phenylated ligand is a side reaction that consumes PhI reagents, being more prominent when less pyrrole is available.

On the other hand, when 1 equiv of **1** was mixed with 2 equiv of pyrrole, an excess of base, and PhI, we observed complete consumption of pyrrole to afford the coupling product in 100% yield; a second addition of 2 equiv of pyrrole also led to full conversion (Figure 4).

To shed more light on the interaction between **1** and the various reaction components, we performed CV measurements in DMSO looking for redox peaks of new species formed in solution under single-turnover conditions. The CV signals of the reactions were taken after stirring the mixtures at 80 °C for 4 h and then adding $LiClO_4$ as electrolyte in the mixture cooled to RT (see the SI for further details). Indeed, when voltammograms were recorded directly after mixing the reagents at RT, no change compared to the CV of **1** was observed, meaning that catalyst activation requires higher temperatures. The CV of the coupling reaction (1) (Scheme 2) shows that the $Cu^{II} \rightarrow Cu^{I}$ reduction peaks at negative potentials disappear while new peaks show up in the positive region of the voltammogram, compatible with $Cu^{II} \rightarrow Cu^{III}$ oxidation of the different copper centers in a distorted coordination environment[63] (see below for intermediates of the proposed catalytic cycle) (Figure 5a). Assignment of these peaks to the formation of phenoxyl radicals on the sal moieties instead of oxidation of the metal center, in comparison to salen derivatives,[64−66] should instead be safely discharged since electron-donor groups able to stabilize the radical are usually required. Additionally, they usually show oxidation peaks in the CV of the copper(II) complexes,[64] a behavior that is not observed with the salben complexes (see Figure S3 in SI), where no oxidation peak is present. The outcome of the radical trap experiment (Scheme 6) further supports the absence of radical species during the catalytic cycle.

https://doi.org/10.1021/acs.organomet.5c00412
Organometallics 2025, 44, 2807−2819

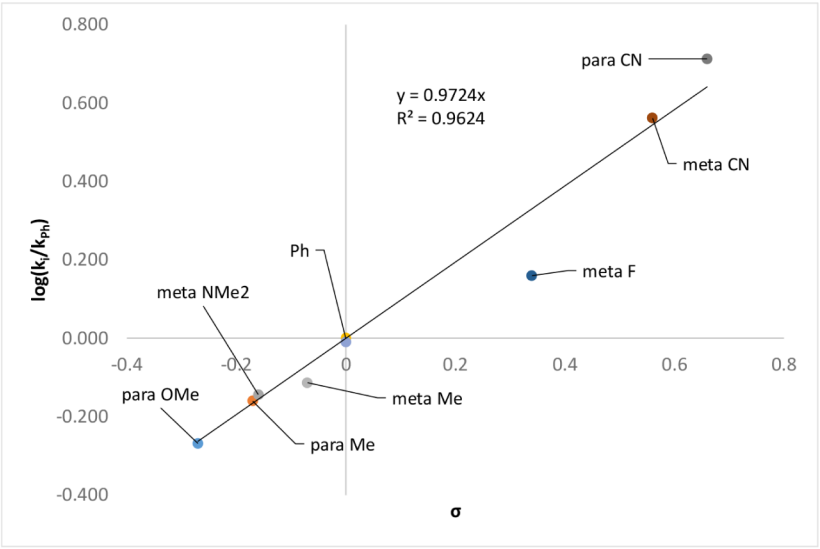

Figure 6. Hammett plot for the coupling of pyrrole with substituted PhI.

Scheme 7. Proposed Catalytic Cycle

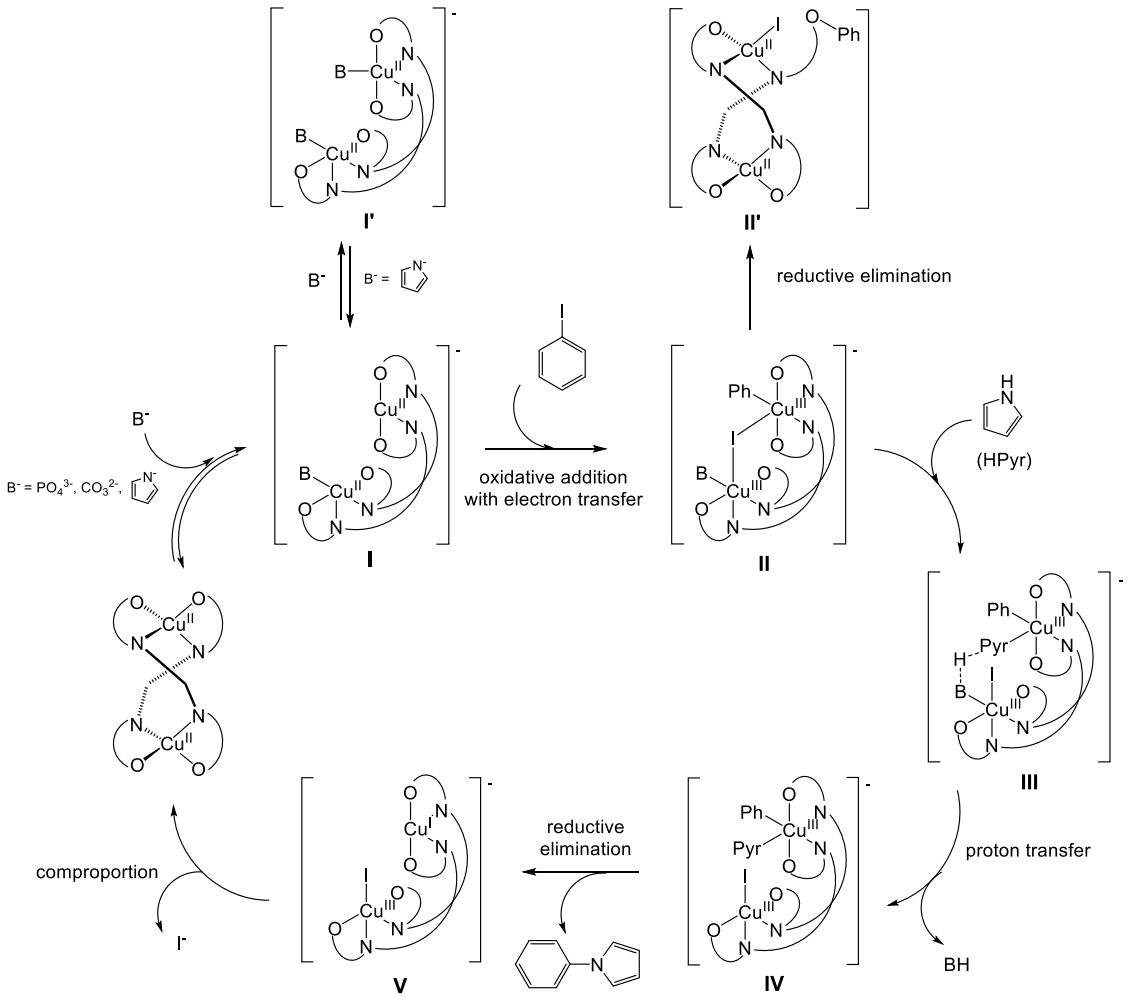

To discern the contribution of each individual reactant of the mixture in altering the redox behavior of the catalyst, we then performed CV measurements of the reaction between **1** and K_3PO_4, **1** and pyrrole, and **1** and PhI. The reaction between **1** and base (Figure 5b) highlighted that there is only one weak peak in the reduction range at the same potential as the second peak of the complex as it is, while it is possible to observe a new couple of quasi-reversible peaks (+0.20 V and +0.46 V for **1** + base; + 0.18 V and +0.53 V for the full model reaction) in the oxidation range that partly overlaps with the

https://doi.org/10.1021/acs.organomet.5c00412
Organometallics 2025, 44, 2807−2819

pair seen in the full model reaction. This supports the idea that the base may coordinate to copper(II), generating a new species prone to oxidation in solution to copper(III). The reaction between **1** and pyrrole (Figure 5c) still shows two peaks in the negative range with a shift of the redox potential of the first reduction from −0.51 V to −0.62 V, while the second reduction does not vary. The shift of the reduction peak may be caused by the interaction of pyrrole with the copper complex. Anyway, the intensity of the peaks of **1** + pyrrole is lower than that of **1** alone. No peak in the oxidation region is present. When the reaction is repeated by adding the base together with pyrrole (Figure 5d), there is the appearance of the oxidation peaks as observed in the CV of the model reaction (Figure 5a).

The reaction between **1** and PhI (Figure 5e) highlighted that there are two peaks for $Cu^{II} \rightarrow Cu^{I}$ in the negative range with a shift of the redox potentials to −0.59 and −0.98 V. On the other hand, additional peaks appear in the oxidation range (+0.32 V and +0.50 V for **1** + PhI), which are absent in the catalyst alone. The CV partially resembles the CVs of the full reaction and of **1** + base. The addition of base to the mixture of **1** + PhI results in a CV (Figure 5f) where the oxidation peaks are well-defined and the reduction peaks almost disappear. This agrees with the stoichiometric experiment showing that in the presence of the base the PhI is consumed faster.

Next, we measured the reaction order for each reactant, using the coupling of pyrrole and PhI with Cs_2CO_3 in MeCN as a reference reaction. The reaction is clearly first-order in PhI and catalyst (Figures S9 and S11 in SI) while pyrrole displays a first-order reaction up to 0.3 mol/L concentration and then turns to a negative order, suggestive of an inhibition effect becoming predominant (Figure S36 in SI). Measuring the order in Cs_2CO_3 did not provide interpretable data, likely due to the challenge associated with the heterogeneous nature of the base; variation of the initial rates may be associated with a high experimental error (Figure S38 in SI). Anyway, the limited solubility of Cs_2CO_3 in MeCN is expected to generate a constant base concentration in solution, providing limited information on the reaction order. The reaction order in the ligand is instead substantially zero, meaning that there is no ligand detachment or disruption of the dinuclear entities during or before the rate determining step (Figure S40 in SI).

Additionally, we determined the Hammett equation for the coupling reaction by measuring the reaction rate of various substituted aryl iodides with pyrrole. As displayed in Figure 6, a good linear correlation across the various substituents is observed, hinting at a consistent mechanism across substrates with different stereoelectronic properties. The positive ρ value of almost 1 (0.9724, R^2 = 0.9624) indicates a buildup of negative charge during the rate-determining step, supportive of the oxidative addition of the C−I bond onto the copper center.

Based on all of the observations collected, the following mechanism can be proposed (Scheme 7). In the first step, the base or the deprotonated pyrrole coordinates to the catalyst to give intermediate **I**, in which one copper center is pentacoordinate. The propensity of the copper centers to give rise to a fifth interaction in their coordination sphere is indeed also observed in the crystal structures, where dimeric units are formed and one of the two copper(II) centers interacts with the phenoxido oxygen atom of an adjacent molecule. Then, PhI oxidatively adds into the second copper(II) center, with concomitant electron transfer from the first one, yielding the copper(III)−copper(III) species **II**. One copper(II) ion, thus, acts as an electron reservoir, in analogy to redox-active ligands.[18,67] Importantly,[18] the propensity of the copper(II) center to undergo oxidative addition may be strongly enhanced by the dianionic nature of the salben ligand. In intermediate **II**, one metal center brings the Ph^-, the second, the base, and the iodido ligand can bridge both metal centers, reaching hexacoordination for both ions and stabilizing the +3 oxidation state, as observed for cobalt.[24] Importantly, intermediate **I** can be coordinated by a second molecule of pyrrolate, generating the saturated species **I′** that cannot undergo phenyl iodide oxidative addition. This agrees with the reaction order observed for the pyrrole, which suggests an inhibition effect for a high concentration of pyrrole (above 0.3 mol L^{-1}). It is important to note that the extent of this inhibiting side reaction is expected to vary depending on the coordination ability of the *N*-nucleophile or its deprotonated form. In the third step of the catalytic cycle, the pyrrole (and in general the *N*-nucleophile) coordinates to one copper(III) center with concomitant deprotonation through the coordinated base or pyrrolate yielding **III**, followed by a shift of the iodide to bind a single copper center, affording intermediate **IV** with one pentacoordinated copper(III) center and the other hexacoordinated one. Finally, *N*-phenylpyrrole is reductively eliminated from the copper center, giving a latent mixed-valence $Cu^{I}-Cu^{III}$ complex (**V**), which immediately comproportionates and releases the iodido anion to regenerate the $Cu^{II}-Cu^{II}$ catalyst **1**. The mechanistic study also highlights a potential off-cycle pathway that originates from intermediate **II**, where the reductive elimination between the phenyl fragment and the oxygen atom of the salben ligand generates species **II′**.

CONCLUSIONS

In summary, we present here well-defined, air-stable, and easily prepared dinuclear copper salben complexes as efficient catalysts for the C−N coupling reactions of aryl iodides. A key feature of these compounds is their superior catalytic performance with *ortho*-substituted derivatives, a substrate class that still represents a challenge and where copper salben derivatives outperform the few catalytic systems previously published, allowing for efficient coupling at a 5- to 10-fold lower copper loading. Additionally, a broad range of *N*-nucleophiles are tolerated, including 5-member *N*-heterocycles—where the catalytic performance of our copper complexes rivals that of the second-generation catalysts—amides, sulfonamides, and amines. It is important to note that this versatility is an uncommon feature among copper-based catalytic systems, where different classes of *N*-nucleophiles usually require different ligands to maximize the coupling efficiency. Mechanistic insights were collected by single-turnover experiments, kinetic studies, and CV measurements and support an atypical mechanism based on an overall nonradical $Cu^{II}-Cu^{III}$ redox couple, where the oxidative addition/reductive elimination events take place on one copper center, while the other copper center acts as an electron reservoir by giving and accepting electrons in tandem with the redox changes on the former. We believe that the distorted geometry imparted by the salben ligand to the copper(II) metal centers, together with its flexibility in adapting to different coordination geometries, plays a key role in enabling access to and stabilization of various oxidation states, a feature eventually leading to high catalytic performances. Additional research is ongoing in our laboratories to

https://doi.org/10.1021/acs.organomet.5c00412
Organometallics 2025, 44, 2807−2819

fully exploit the potential of this novel class of catalysts and their mechanism of action.

EXPERIMENTAL SECTION

General Information for Synthesis and Structural Characterization. All chemicals were reagent grade, and solvents were used as received. Elemental analyses were performed with a Thermo Scientific Flash 2000 (CHNS analyzer) instrument. ^{1}H and ^{13}C NMR spectra were recorded on a Bruker FT-NMR Advance 400 spectrometer at room temperature (RT) (^{1}H: 400 MHz; ^{13}C, 101 MHz). Proton and carbon chemical shifts are given in parts per million (ppm) versus external TMS, and they were determined by reference to the solvent residual signals (^{1}H NMR: 7.26 ppm, ^{13}C NMR: 77.0 ppm for $CDCl_3$; ^{1}H NMR: 2.05 ppm, ^{13}C NMR: 29.8 ppm for acetone-d_6); coupling constants are given in Hz. Infrared spectra were recorded as ATR spectra using a Jasco FTIR-4700LE spectrophotometer equipped with a diamond tip for solids and with a 2 cm^{-1} resolution; bands are reported as wavenumbers (cm^{-1}) with their assignments and relative intensity (vs = very strong, s = strong, *m* = medium, w = weak, br = broad). The MS-ESI^{+} measurements were performed using the Agilent 6300 Ion Trap LC/MS mass spectrometer through the Electrospray Ionization (ESI) method, dissolving the sample in MeOH (1 mg/1 mL) and diluting with MeOH to 10 ppm before injection. H_2L^1, H_2L^2, H_2L^3, H_2L^4, and H_2L^5 were synthesized as previously reported.[23] Single crystals suitable for X-ray diffraction of H_2L^2 were obtained by the slow evaporation of a solution of the ligand in $CHCl_3$. **1** and **5** were obtained as previously reported.[22] Single crystals of **5** suitable for X-ray diffraction were obtained by the slow diffusion of *n*-hexane into a solution of the title compound in dichloromethane (DCM). Further details on the synthesis of ligands and complexes, structural data, and all catalytic experiments can be found in SI.

ASSOCIATED CONTENT

Supporting Information

The Supporting Information is available free of charge at https://pubs.acs.org/doi/10.1021/acs.organomet.5c00412.

Experimental section for synthesis, structural, and CV characterizations of ligands and copper complexes; X-ray crystal structure determination; description of CV measurements; experimental section for catalysis; NMR yield with internal standard; optimization of reaction conditions for the model reaction; general procedure for the coupling reactions to products **8b−8p** and **9a−9h**; isolation and characterization of products; procedure for the scale-up of coupling reactions; ^{1}H NMR in $CDCl_3$ of the crude reaction mixture with Me_2SO_2 as internal standard; calibration procedure for HPLC quantitative analysis experiments; procedure for single-turnover experiments; reaction of PhI with **1** in the absence of base for detection of phenylated salben ligand; reaction order experiments; and initial rates analysis for the Hammett correlation (PDF)

Accession Codes

Deposition Numbers 2465895−2465898, 2477654, 2477656−2477657, 2477677, and 2478326 contain the supplementary crystallographic data for this paper. These data can be obtained free of charge via the joint Cambridge Crystallographic Data Centre (CCDC) and Fachinformationszentrum Karlsruhe Access Structures service.

AUTHOR INFORMATION

Corresponding Authors

Luca Rigamonti − *Dipartimento di Scienze Chimiche e Geologiche, Università Degli Studi di Modena e Reggio Emilia, Modena 41125, Italy;* orcid.org/0000-0002-9875-9765; Email: luca.rigamonti@unimore.it

Serena Maria Fantasia − *Synthetic Molecules Technical Development, Process Chemistry & Catalysis, F. Hoffmann-La Roche Ltd, Basel CH-4070, Switzerland;* Email: serena_maria.fantasia@roche.com

Authors

Lorenzo Marchi − *Dipartimento di Scienze Chimiche e Geologiche, Università Degli Studi di Modena e Reggio Emilia, Modena 41125, Italy; Synthetic Molecules Technical Development, Process Chemistry & Catalysis, F. Hoffmann-La Roche Ltd, Basel CH-4070, Switzerland*

Luca Terraneo − *Synthetic Molecules Technical Development, Process Chemistry & Catalysis, F. Hoffmann-La Roche Ltd, Basel CH-4070, Switzerland*

Gabriele Vaccari − *Dipartimento di Scienze Chimiche e Geologiche, Università Degli Studi di Modena e Reggio Emilia, Modena 41125, Italy; Synthetic Molecules Technical Development, Process Chemistry & Catalysis, F. Hoffmann-La Roche Ltd, Basel CH-4070, Switzerland*

Markus Steiner − *Synthetic Molecules Technical Development, Process Chemistry & Catalysis, F. Hoffmann-La Roche Ltd, Basel CH-4070, Switzerland*

Ritik Singhal − *Synthetic Molecules Technical Development, Process Chemistry & Catalysis, F. Hoffmann-La Roche Ltd, Basel CH-4070, Switzerland*

Laura Pigani − *Dipartimento di Scienze Chimiche e Geologiche, Università Degli Studi di Modena e Reggio Emilia, Modena 41125, Italy*

Carlo Castellano − *Dipartimento di Chimica, Università Degli Studi di Milano, Milano 20133, Italy;* orcid.org/0000-0002-7497-0670

Francesco Demartin − *Dipartimento di Chimica, Università Degli Studi di Milano, Milano 20133, Italy*

Philipp Pascal Nievergelt − *Pharma Research and Early Development, Roche Innovation Center Basel, F. Hoffmann-La Roche Ltd, Basel CH-4070, Switzerland*

André Alker − *Pharma Research and Early Development, Roche Innovation Center Basel, F. Hoffmann-La Roche Ltd, Basel CH-4070, Switzerland*

Frank Stowasser − *Pharma Research and Early Development, Roche Innovation Center Basel, F. Hoffmann-La Roche Ltd, Basel CH-4070, Switzerland*

Complete contact information is available at: https://pubs.acs.org/10.1021/acs.organomet.5c00412

Notes

The authors declare no competing financial interest.

ACKNOWLEDGMENTS

L.R. and S.M.F. extend their gratitude to Prof. Alessandro Pasini, their PhD mentor at the University of Milan, for his invaluable support and guidance in mastering the art of research. L.M. and L.R. would like to thank the Dipartimento di Scienze Chimiche e Geologiche of the Università degli Studi di Modena e Reggio Emilia for the financial support through the Fondo Dipartimentale per la Ricerca 2021 linea dottorato (FDR2021) and F. Hoffmann-La Roche Ltd. for additional financial support. The HORSS team (High Output Reaction Screening System) from F. Hoffmann-La Roche Ltd. is greatly acknowledged for their support with the screening of reaction conditions.

https://doi.org/10.1021/acs.organomet.5c00412
Organometallics 2025, 44, 2807−2819

REFERENCES

(1) Ullmann, F. Ueber Eine Neue Bildungsweise von Diphenylaminderivaten. *Ber. Dtsch. Chem. Ges.* **1903**, *36* (2), 2382−2384.
(2) Goldberg, I. Über Phenylierung von Primären Aromatischen Aminen. *Ber. Dtsch. Chem. Ges.* **1907**, *40* (4), 4541−4546.
(3) Monnier, F.; Taillefer, M. Catalytic C-C, C-N, and C-O Ullmann-Type Coupling Reactions. *Angew. Chem., Int. Ed.* **2009**, *48* (38), 6954−6971.
(4) Yang, Q.; Zhao, Y.; Ma, D. Cu-Mediated Ullmann-Type Cross-Coupling and Industrial Applications in Route Design, Process Development, and Scale-up of Pharmaceutical and Agrochemical Processes. *Org. Process Res. Dev.* **2022**, *26* (6), 1690−1750.
(5) Zhou, W.; Fan, M.; Yin, J.; Jiang, Y.; Ma, D. CuI/Oxalic Diamide Catalyzed Coupling Reaction of (Hetero)Aryl Chlorides and Amines. *J. Am. Chem. Soc.* **2015**, *137* (37), 11942−11945.
(6) De, S.; Yin, J.; Ma, D. Copper-Catalyzed Coupling Reaction of (Hetero)Aryl Chlorides and Amides. *Org. Lett.* **2017**, *19* (18), 4864−4867.
(7) Li, Q.; Xu, L.; Ma, D. Cu-Catalyzed Coupling Reactions of Sulfonamides with (Hetero)Aryl Chlorides/Bromides. *Angew. Chem., Int. Ed.* **2022**, *61* (43), No. e202210483.
(8) Li, S.; Xu, L.; An, B.; Ma, D. Assembly of Biaryl Amines via Mild Copper-Catalyzed Coupling of Anilines with (Hetero)Aryl Chlorides/Bromides. *Org. Lett.* **2025**, *27* (6), 1498−1503.
(9) Ray, R.; Hartwig, J. F. Oxalohydrazide Ligands for Copper-Catalyzed C−O Coupling Reactions with High Turnover Numbers. *Angew. Chem., Int. Ed.* **2021**, *60* (15), 8203−8211.
(10) Pierson, C. N.; Horak, T.; Amberg, W. M.; Ray, R.; Rao, G.; Pinkhassik, T. M.; Fantasia, S. M.; Rummelt, S. M.; Püntener, K.; Britt, R. D.; Hartwig, J. F. Efficient Aminations of Aryl Halides by a Cu(II) Catalyst. *J. Am. Chem. Soc.* **2025**, *147* (24), 20939−20946.
(11) Kim, S.-T.; Strauss, M. J.; Cabré, A.; Buchwald, S. L. Room-Temperature Cu-Catalyzed Amination of Aryl Bromides Enabled by DFT-Guided Ligand Design. *J. Am. Chem. Soc.* **2023**, *145* (12), 6966−6975.
(12) Strauss, M. J.; Liu, K. X.; Greaves, M. E.; Dahl, J. C.; Kim, S.-T.; Wu, Y.-J.; Schmidt, M. A.; Scola, P. M.; Buchwald, S. L. Cu-Catalyzed Amination of Base-Sensitive Aryl Bromides and the Chemoselective N- and O-Arylation of Amino Alcohols. *J. Am. Chem. Soc.* **2024**, *146* (27), 18616−18625.
(13) Düker, J.; Petersen, N.; Richter, N.; Feuerer, P.; Faber, T.; Hölter, N.; Kehl, N.; Oboril, J.; Strippel, J.; Gröer, A.; Guimond, N.; Kaldas, S. J.; Lübbesmeyer, M.; Volpin, G.; König, B.; Hillenbrand, J. Room-Temperature Copper Cross-Coupling Reactions of Anilines with Aryl Bromides. *Org. Lett.* **2025**, *27* (22), 5566−5571.
(14) Ruiz-Castillo, P.; Buchwald, S. L. Applications of Palladium-Catalyzed C−N Cross-Coupling Reactions. *Chem. Rev.* **2016**, *116* (19), 12564−12649.
(15) Gildner, P. G.; Colacot, T. J. Reactions of the 21st Century: Two Decades of Innovative Catalyst Design for Palladium-Catalyzed Cross-Couplings. *Organometallics* **2015**, *34* (23), 5497−5508.
(16) Campeau, L.-C.; Hazari, N. Cross-Coupling and Related Reactions: Connecting Past Success to the Development of New Reactions for the Future. *Organometallics* **2019**, *38* (1), 3−35.
(17) Sambiagio, C.; Marsden, S. P.; Blacker, A. J.; McGowan, P. C. Copper Catalysed Ullmann Type Chemistry: From Mechanistic Aspects to Modern Development. *Chem. Soc. Rev.* **2014**, *43* (10), 3525−3550.
(18) Delaney, C. P.; Lin, E.; Huang, Q.; Yu, I. F.; Rao, G.; Tao, L.; Jed, A.; Fantasia, S. M.; Püntener, K. A.; Britt, R. D.; Hartwig, J. F. Cross-Coupling by a Noncanonical Mechanism Involving the Addition of Aryl Halide to Cu(II). *Science* **2023**, *381* (6662), 1079−1085.
(19) Yadav, K. K.; Narang, U.; Bhattacharya, S.; Chauhan, S. M. S. CopperII Phthalocyanine as an Efficient and Reusable Catalyst for the N-Arylation of Nitrogen Containing Heterocycles. *Tetrahedron Lett.* **2017**, *58* (31), 3044−3048.
(20) Talukdar, V.; Mondal, K.; Halder, P.; Das, P. Ullmann-Type *N* -, *S* -, and *O* -Arylation Using a Well-Defined 7-Azaindole- *N* -Oxide (7-AINO)-Based Copper(II) Catalyst: Scope and Application to Drug Synthesis. *J. Org. Chem.* **2024**, *89* (11), 7455−7471.
(21) Beletskaya, I. P.; Cheprakov, A. V. Copper in Cross-Coupling Reactions. *Coord. Chem. Rev.* **2004**, *248* (21−24), 2337−2364.
(22) Pasini, A.; Demartin, F.; Piovesana, O.; Chiari, B.; Cinti, A.; Crispu, O. Novel Copper(II) Complexes of "Short" Salen Homologues. Structure and Magnetic Properties of the Tetranuclear Complex $[Cu_2(L^2)_2]_2$ [H_2L^2 = Phenyl-*N*,*N* ′-Bis(Salicylidene)-Methanediamine]. *J. Chem. Soc., Dalton Trans.* **2000**, No. 19, 3467−3472.
(23) Takajo, T.; Kambe, S.; Ando, W. Synthesis of *N*,*N*′-Bis[2-Hydroxybenzylidene]Arylmethanediamines. *Synthesis* **1984**, *1984* (3), 256−259.
(24) Chiari, B.; Cinti, A.; Crispu, O.; Demartin, F.; Pasini, A.; Piovesana, O. Binuclear Co(II)Co(II), Co(II)Co(III) and Co(III)-Co(III) Complexes of "Short" Salen Homologues Derived from the Condensation of Salicylaldehyde and Methanediamine or Phenylmethanediamines. Synthesis, Structures and Magnetism. *J. Chem. Soc., Dalton Trans.* **2001**, No. 24, 3611−3616.
(25) Chiari, B.; Cinti, A.; Crispu, O.; Demartin, F.; Pasini, A.; Piovesana, O. New Pentanuclear Mixed Valence Co(II)−Co(III) Complexes of "Short" Salen Homologues. *J. Chem. Soc., Dalton Trans.* **2002**, No. 24, 4672−4677.
(26) Rigamonti, L.; Zardi, P.; Carlino, S.; Demartin, F.; Castellano, C.; Pigani, L.; Ponti, A.; Ferretti, A. M.; Pasini, A. Selective Formation, Reactivity, Redox and Magnetic Properties of Mn^{III} and Fe^{III} Dinuclear Complexes with Shortened Salen-Type Schiff Base Ligands. *Int. J. Mol. Sci.* **2020**, *21* (21), 7882.
(27) Marchi, L.; Carlino, S.; Castellano, C.; Demartin, F.; Forni, A.; Ferretti, A. M.; Ponti, A.; Pasini, A.; Rigamonti, L. Substituent-Guided Cluster Nuclearity for Tetranuclear Iron(III) Compounds with Flat $\{Fe_4(\mu_3\text{-}O)_2\}$ Butterfly Core. *Int. J. Mol. Sci.* **2023**, *24* (6), 5808.
(28) Cozzi, P. G. Metal−Salen Schiff Base Complexes in Catalysis: Practical Aspects. *Chem. Soc. Rev.* **2004**, *33* (7), 410−421.
(29) Lo, Q. A.; Sale, D.; Braddock, D. C.; Davies, R. P. Mechanistic and Performance Studies on the Ligand-Promoted Ullmann Amination Reaction. *ACS Catal.* **2018**, *8* (1), 101−109.
(30) Giri, R.; Hartwig, J. F. Cu(I)−Amido Complexes in the Ullmann Reaction: Reactions of Cu(I)−Amido Complexes with Iodoarenes with and without Autocatalysis by CuI. *J. Am. Chem. Soc.* **2010**, *132* (45), 15860−15863.
(31) Cristau, H.-J.; Cellier, P. P.; Spindler, J.-F.; Taillefer, M. Highly Efficient and Mild Copper-Catalyzed N- and C-Arylations with Aryl Bromides and Iodides. *Chem. − Eur. J.* **2004**, *10* (22), 5607−5622.
(32) Cristau, H.; Cellier, P. P.; Spindler, J.; Taillefer, M. Mild Conditions for Copper-Catalysed *N* -Arylation of Pyrazoles. *Eur. J. Org. Chem.* **2004**, *2004* (4), 695−709.
(33) Ouali, A.; Taillefer, M.; Spindler, J.-F.; Jutand, A. Precatalysts Involved in Copper-Catalyzed Arylations of Nucleophiles. *Organometallics* **2007**, *26* (1), 65−74.
(34) Dewan, A.; Bora, U.; Borah, G. A Simple and Efficient Tetradentate Schiff Base Derived Palladium Complex for Suzuki−Miyaura Reaction in Water. *Tetrahedron Lett.* **2014**, *55* (10), 1689−1692.
(35) Gogoi, A.; Sarmah, G.; Dewan, A.; Bora, U. Unique Copper−Salen Complex: An Efficient Catalyst for N-Arylations of Anilines and Imidazoles at Room Temperature. *Tetrahedron Lett.* **2014**, *55* (1), 31−35.
(36) Sharghi, H.; Aberi, M.; Shiri, P. Highly Reusable Support-free Copper(II) Complex of *Para* -hydroxy-substituted Salen: Novel, Efficient and Versatile Catalyst for C−N Bond Forming Reactions. *Appl. Organomet. Chem.* **2017**, *31* (11), No. e3761.
(37) Fantasia, S. M.; Marchi, L.; Rigamonti, L.; Steiner, M. *C-N Coupling Process with $[Cu_2(\mu\text{-Salben})_2]$ Complexes*; WO 2025/016888 A1, 2025.
(38) Kambe, S.; Takajo, T.; Saito, K.; Hayashi, T.; Sakurai, A.; Midorikawa, H. A Simple Synthesis of a New Heterocycle from *N*,*N*′-Bis[2-Hydroxybenzylidene]-2-Hydroxy-α,α-Tolyldiamine and Carbonyl Compounds. *Synthesis* **1975**, *1975* (12), 802−804.

https://doi.org/10.1021/acs.organomet.5c00412
Organometallics 2025, 44, 2807−2819

(39) Yang, L.; Powell, D. R.; Houser, R. P. Structural Variation in Copper(I) Complexes with Pyridylmethylamide Ligands: Structural Analysis with a New Four-Coordinate Geometry Index, τ_4. *Dalton Trans.* **2007**, No. 9, 955−964.
(40) Rigamonti, L.; Demartin, F.; Forni, A.; Righetto, S.; Pasini, A. Copper(II) Complexes of Salen Analogues with Two Differently Substituted (Push−Pull) Salicylaldehyde Moieties. A Study on the Modulation of Electronic Asymmetry and Nonlinear Optical Properties. *Inorg. Chem.* **2006**, *45* (26), 10976−10989.
(41) Samha, M. H.; Karas, L. J.; Vogt, D. B.; Odogwu, E. C.; Elward, J.; Crawford, J. M.; Steves, J. E.; Sigman, M. S. Predicting Success in Cu-Catalyzed C−N Coupling Reactions Using Data Science. *Sci. Adv.* **2024**, *10* (3), No. eadn3478.
(42) Ganesh, B. H.; Raj, A. G.; Aruchamy, B.; Nanjan, P.; Drago, C.; Ramani, P. Pyrrole: A Decisive Scaffold for the Development of Therapeutic Agents and Structure-Activity Relationship. *ChemMedChem* **2024**, *19* (1), No. e202300447.
(43) Vitaku, E.; Smith, D. T.; Njardarson, J. T. Analysis of the Structural Diversity, Substitution Patterns, and Frequency of Nitrogen Heterocycles among U.S. FDA Approved Pharmaceuticals: Miniperspective. *J. Med. Chem.* **2014**, *57* (24), 10257−10274.
(44) Antilla, J. C.; Baskin, J. M.; Barder, T. E.; Buchwald, S. L. Copper−Diamine-Catalyzed *N* -Arylation of Pyrroles, Pyrazoles, Indazoles, Imidazoles, and Triazoles. *J. Org. Chem.* **2004**, *69* (17), 5578−5587.
(45) Larsson, P.; Correa, A.; Carril, M.; Norrby, P.; Bolm, C. Copper-Catalyzed Cross-Couplings with Part-per-Million Catalyst Loadings. *Angew. Chem., Int. Ed.* **2009**, *121* (31), 5801−5803.
(46) Ding, Z.; Nie, N.; Chen, T.; Meng, L.; Wang, G.; Chen, Z.; Hu, J. L-Proline N-Oxide Dihydrazides as an Efficient Ligand for Cross-Coupling Reactions of Aryl Iodides and Bromides with Amines and Phenols. *Tetrahedron* **2021**, *79*, 131826.
(47) Altman, R. A.; Buchwald, S. L. 4,7-Dimethoxy-1,10-Phenanthroline: An Excellent Ligand for the Cu-Catalyzed *N* -Arylation of Imidazoles. *Org. Lett.* **2006**, *8* (13), 2779−2782.
(48) Antilla, J. C.; Klapars, A.; Buchwald, S. L. The Copper-Catalyzed *N* -Arylation of Indoles. *J. Am. Chem. Soc.* **2002**, *124* (39), 11684−11688.
(49) Pawar, G. G.; Wu, H.; De, S.; Ma, D. Copper(I) Oxide/*N*, *N*′ -Bis[(2-furyl)Methyl]oxalamide-Catalyzed Coupling of (Hetero)Aryl Halides and Nitrogen Heterocycles at Low Catalytic Loading. *Adv. Synth. Catal.* **2017**, *359* (10), 1631−1636.
(50) Yang, X.; Xing, H.; Zhang, Y.; Lai, Y.; Zhang, Y.; Jiang, Y.; Ma, D. CuI/8-Hydroxyquinalidine Promoted *N* -Arylation of Indole and Azoles. *Chin. J. Chem.* **2012**, *30* (4), 875−880.
(51) Klapars, A.; Antilla, J. C.; Huang, X.; Buchwald, S. L. A General and Efficient Copper Catalyst for the Amidation of Aryl Halides and the *N* -Arylation of Nitrogen Heterocycles. *J. Am. Chem. Soc.* **2001**, *123* (31), 7727−7729.
(52) Bhunia, S.; Pawar, G. G.; Kumar, S. V.; Jiang, Y.; Ma, D. Selected Copper-Based Reactions for C−N, C−O, C−S, and C−C Bond Formation. *Angew. Chem., Int. Ed.* **2017**, *56* (51), 16136−16179.
(53) Modak, A.; Nett, A. J.; Swift, E. C.; Haibach, M. C.; Chan, V. S.; Franczyk, T. S.; Shekhar, S.; Cook, S. P. Cu-Catalyzed C−N Coupling with Sterically Hindered Partners. *ACS Catal.* **2020**, *10* (18), 10495−10499.
(54) De Gombert, A.; Darù, A.; Ahmed, T. S.; Haibach, M. C.; Li-Matsuura, R.; Yang, C.; Henry, R. F.; Cook, S. P.; Shekhar, S.; Blackmond, D. G. Mechanistic Insight into Cu-Catalyzed C−N Coupling of Hindered Aryl Iodides and Anilines Using a Pyrrol-Ol Ligand Enables Development of Mild and Homogeneous Reaction Conditions. *ACS Catal.* **2023**, *13* (5), 2904−2915.
(55) Yang, K.; Qiu, Y.; Li, Z.; Wang, Z.; Jiang, S. Ligands for Copper-Catalyzed C−N Bond Forming Reactions with 1 Mol% CuBr as Catalyst. *J. Org. Chem.* **2011**, *76* (9), 3151−3159.
(56) Bhunia, S.; De, S.; Ma, D. Room Temperature Cu-Catalyzed *N* -Arylation of Oxazolidinones and Amides with (Hetero)Aryl Iodides. *Org. Lett.* **2022**, *24* (5), 1253−1257.
(57) Beletskaya, I. P.; Cheprakov, A. V. The Complementary Competitors: Palladium and Copper in C−N Cross-Coupling Reactions. *Organometallics* **2012**, *31* (22), 7753−7808.
(58) Chen, Z.; Ma, D. Cu/*N*, *N* ′-Dibenzyloxalamide-Catalyzed *N* -Arylation of Heteroanilines. *Org. Lett.* **2019**, *21* (17), 6874−6878.
(59) Huffman, L. M.; Stahl, S. S. Carbon−Nitrogen Bond Formation Involving Well-Defined Aryl−Copper(III) Complexes. *J. Am. Chem. Soc.* **2008**, *130* (29), 9196−9197.
(60) Casitas, A.; King, A. E.; Parella, T.; Costas, M.; Stahl, S. S.; Ribas, X. Direct Observation of CuI/CuIII Redox Steps Relevant to Ullmann-Type Coupling Reactions. *Chem. Sci.* **2010**, *1* (3), 326−330.
(61) Liu, H.; Shen, Q. Well-Defined Organometallic Copper(III) Complexes: Preparation, Characterization and Reactivity. *Coord. Chem. Rev.* **2021**, *442*, 213923.
(62) Howard, J. K.; Rihak, K. J.; Bissember, A. C.; Smith, J. A. The Oxidation of Pyrrole. *Chem. - Asian J.* **2016**, *11* (2), 155−167.
(63) Blusch, L. K.; Craigo, K. E.; Martin-Diaconescu, V.; McQuarters, A. B.; Bill, E.; Dechert, S.; DeBeer, S.; Lehnert, N.; Meyer, F. Hidden Non-Innocence in an Expanded Porphyrin: Electronic Structure of the Siamese-Twin Porphyrin's Dicopper Complex in Different Oxidation States. *J. Am. Chem. Soc.* **2013**, *135* (37), 13892−13899.
(64) Orio, M.; Jarjayes, O.; Kanso, H.; Philouze, C.; Neese, F.; Thomas, F. X-Ray Structures of Copper(II) and Nickel(II) Radical Salen Complexes: The Preference of Galactose Oxidase for Copper-(II). *Angew. Chem., Int. Ed.* **2010**, *49* (29), 4989−4992.
(65) Storr, T.; Verma, P.; Pratt, R. C.; Wasinger, E. C.; Shimazaki, Y.; Stack, T. D. P. Defining the Electronic and Geometric Structure of One-Electron Oxidized Copper−Bis-Phenoxide Complexes. *J. Am. Chem. Soc.* **2008**, *130* (46), 15448−15459.
(66) Takeyama, T.; Suzuki, T.; Kikuchi, M.; Kobayashi, M.; Oshita, H.; Kawashima, K.; Mori, S.; Abe, H.; Hoshino, N.; Iwatsuki, S.; Shimazaki, Y. Solid State Characterization of One- and Two-Electron Oxidized Cu^{II} -salen Complexes with *Para* -Substituents: Geometric Structure-Magnetic Property Relationship. *Eur. J. Inorg. Chem.* **2021**, *2021* (39), 4133−4145.
(67) Lyaskovskyy, V.; De Bruin, B. Redox Non-Innocent Ligands: Versatile New Tools to Control Catalytic Reactions. *ACS Catal.* **2012**, *2* (2), 270−279.

https://doi.org/10.1021/acs.organomet.5c00412
Organometallics 2025, 44, 2807−2819